Matrix Isolation Studies on Alkali-metal Phosphites, Arsenites, and Antimonites. The Characterisation of Molecular $NaPO_2$, $CsAsO_2$, and $KSbO_2$

By J. Steven Ogden * and Stephen J. Williams, Department of Chemistry, The University, Southampton SO9 5NH

Infrared spectra have been obtained for some molecular species MPO_2, $MAsO_2$, and $MSbO_2$ (M = alkali metal) isolated in nitrogen matrices, and three of these species are characterised in detail. For $NaPO_2$, fundamentals are observed at 1 062.1, ν(P–O), 1 151.6, ν(P–O), and 523.0 $\delta(PO_2)$ cm^{-1}, whilst in $CsAsO_2$ and $KSbO_2$, corresponding modes are observed at 863.0, 851.5, and 393.0 cm^{-1} and at 764.6, 744.8, and 339.0 cm^{-1} respectively. ^{18}O-enrichment experiments indicate C_{2v} ring structures for all three MXO_2 species, and bond angles are estimated as OPO = 114, OAsO = 115, and OSbO = 106°.

THE combination of matrix isolation and i.r. spectroscopy is now well established as a method of characterising new high-temperature chemical species, and we are currently using these techniques to investigate a wide range of oxo-anion salts.[1] In particular, we have shown that molecular $NaPO_3$ is an important species produced in the vaporisation of sodium orthophosphate (Na_3PO_4) or trimetaphosphate ($Na_5P_3O_{10}$) from platinum containers,[2,3] and established both its shape and several of its vibrational fundamentals. However, the use of molybdenum or tantalum sample holders in these experiments has recently been shown to give rise to a second species which has qualitatively been identified as $NaPO_2$. A preliminary report of this work has appeared elsewhere,[3] and one of the purposes of this present paper is to discuss the spectra of this species in more detail, and to report similar studies on other alkali-metal phosphate systems.

Virtually nothing is known about the corresponding arsenic and antimony species, and the remainder of this paper describes our matrix i.r. results on a range of alkali-metal As and Sb oxo-salts such as $KAsO_2$.

EXPERIMENTAL

The phosphate samples used in these experiments were obtained by two general routes. For the lithium, sodium, and potassium systems, all the salts were obtained commercially and used without further purification. In the case of the remaining rubidium and caesium systems, phosphate samples were prepared either in situ or beforehand by heating a 1 : 1 mixture of the anhydrous carbonate with P_2O_5 until there was no further evolution of CO_2.[4] This synthetic route was also used to prepare samples of sodium and potassium phosphates to confirm that the same spectral results could be obtained as from the commercial materials. Samples of ^{18}O-enriched sodium phosphate were prepared by oxidation of the phosphide as described in our earlier paper,[2] and in all the phosphate experiments discussed here samples were mixed with tantalum powder prior to vaporisation.

For the arsenic and antimony systems, the starting materials were typically either commercially available salts such as $KAsO_2$, $NaAsO_2$, or $KSb(OH)_6$, or 1 : 1 mixtures of the anhydrous carbonate with As_2O_3 or Sb_2O_3. These mixtures similarly evolved CO_2 on heating and ultimately yielded spectra which were identical to those from the

corresponding commercial salts. Oxygen-18 enrichment in these systems was conveniently carried out by water exchange. Here, a weighed sample of either the commercial salt or the product of a carbonate/oxide fusion reaction was allowed to stand in contact with $H_2^{18}O$ (typically 1.0 cm^3, 90 atom % ^{18}O) in a sealed tube for several days, at room temperature. After removal of water, the solid remaining ultimately yielded spectra which showed that oxygen exchange had taken place.

The general features of our matrix isolation apparatus have been described elsewhere.[5] For this work, samples were typically vaporised from a small platinum boat contained inside an alumina holder fitted with an inductively heated tantalum sleeve. Sample temperatures during deposition were monitored using an optical pyrometer, and matrix gas flows were regulated with a fine-control needle valve. The matrix gases used in these experiments were high purity nitrogen and argon (BOC 99.999%), but nitrogen was found to give superior spectra for all systems, and all the results discussed in this paper refer to nitrogen matrices.

Normal deposition times were typically 30—60 min, and during this period, the central CsI window in our cryostat was maintained at ca. 12 K and the matrix ratio maintained at >1 000 : 1. However, a few experiments were carried out using very rapid deposition times (ca. 15—20 min) with lower matrix ratios in an attempt to identify polymeric species, and controlled diffusion studies up to ca. 35 K were also performed. Infrared spectra were recorded on a Perkin-Elmer 225 IR spectrometer (200—5 000 cm^{-1}) and calibrated using standard procedures.

RESULTS AND DISCUSSION

MPO_2 Species.—In our earlier note on the identification of molecular $NaPO_2$, we indicated how this molecule could be produced as a result of heating a mixture of sodium phosphate ($Na_5P_3O_{10}$) and tantalum powder in vacuo at ca. 1 500 K.[3] Subsequent trapping in a nitrogen matrix led to its characterisation by i.r. spectroscopy, and a C_{2v} ring structure was proposed on the basis of ^{16}O/^{18}O isotope patterns in the P–O stretching region. The experiments described here extend these studies to include the complete range of common alkali metals (Li→Cs), and also extend the spectral range into the far-i.r. in a search for the remaining vibrational fundamentals.
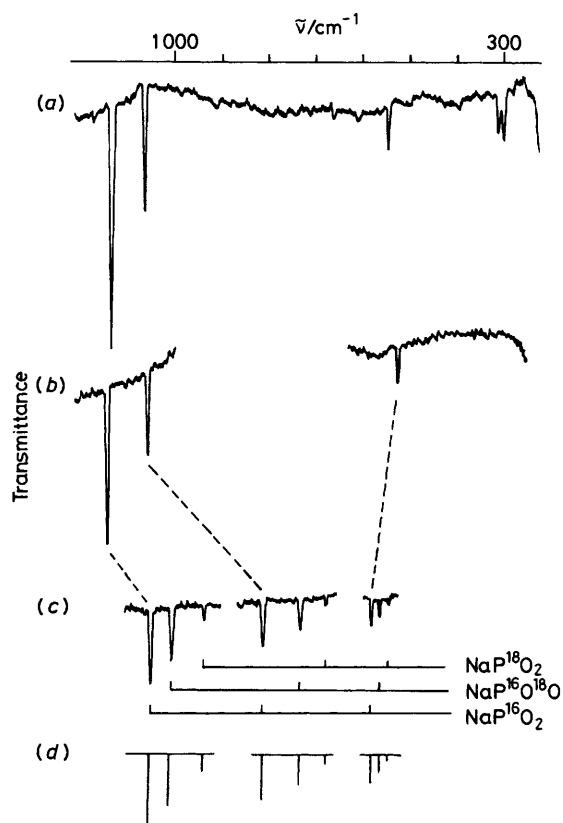
Figure 1(a) shows a typical nitrogen matrix spectrum

FIGURE 1   (a) N_2 matrix i.r. spectrum obtained from vaporisation of Li_3PO_4–Ta. (b) N_2 matrix i.r. spectrum obtained from $Na_5P_3O_{10}$–Ta. (c) Isotope patterns observed for matrix-isolated $NaPO_2$ (ca. 26 atom % ^{18}O enrichment). (d) Calculated spectrum

(1 200—250 cm^{-1}) obtained from the vaporisation of a (1 : 1) Li_3PO_4–Ta mixture at ca. 1 750 K. This spectrum shows prominent absorptions in the P–O stretching region (1 000—1 200 cm^{-1}) and at ca. 530 cm^{-1}, and also two bands at 302 and 311 cm^{-1}. Analogous experiments

on sodium phosphate systems (Na_3PO_4–Ta or $Na_5P_3O_{10}$–Ta) produced three bands at 1 151.6, 1 062.1, and 523.0 cm^{-1}, and similar spectra were also obtained from prepared samples of potassium, rubidium, and caesium phosphates. However, only the Li system gave absorptions at ca. 300 cm^{-1}. The results obtained from a range of alkali-metal phosphate systems are summarised in Table 1, where it is evident that three bands at ca. 1 150, ca. 1 060, and ca. 520 cm^{-1} are common to all phosphate–tantalum mixtures. Some of these systems were also studied in argon matrices, but these spectra were generally of poorer quality, with bands often showing complex structure which may be attributed to multiple site trapping.[6] The general positions of these bands, however, were very similar to the singlet absorptions observed in nitrogen.

On the basis of our earlier characterisation of $NaPO_2$, the bands in Table 1 are assigned as fundamentals of the PO_2 unit in a general C_{2v} structure $M\overset{O}{\underset{O}{<}}{>}P$, where M represents the alkali metal. For this structure, $\Gamma_{vib.} = 3A_1 + B_1 + 2B_2$ with the PO_2 unit contributing three in-plane modes with symmetries A_1(stretch), B_2(stretch), and A_1(bend). A preliminary identification of these modes may be made by reference to SO_2 (which is isoelectronic with PO_2^-) and to the C_{2v} ion $H_2PO_2^-$. In SO_2, the three fundamentals occur[7] at 1 151.4 (A_1), 1 361.8 (B_2), and 517.7 cm^{-1} (A_1), whilst in $H_2PO_2^-$ the corresponding PO_2 modes lie[8] at 1 046, 1 180, and 470 cm^{-1}. Comparison of these frequencies with the data in Table 1 leads to the proposed assignments, and these were subsequently confirmed by ^{18}O-enrichment experiments.

The remaining $A_1 + B_1 + B_2$ modes result from cation motion. Two of these ($A_1 + B_2$) may be approximately described as M–O stretching modes, whilst the B_1 vibration corresponds to an out-of-plane deformation. By analogy with other systems[2] in which alkali-metal–oxygen modes have been assigned,

TABLE 1

Infrared vibrational frequencies (cm^{-1}) for matrix-isolated MXO_2 species

		Assignments [a]		
System	Species	$\nu(X-O)$, B_2	$\nu(X-O)$, A_1	$\delta(XO_2)$, A_1
Li_3PO_4–Ta	$LiPO_2$	1 134.8	1 064.0	546.2
Na_3PO_4–Ta $Na_5P_3O_{10}$–Ta $Na_4P_2O_7$–Ta	$NaPO_2$	1 151.6	1 062.1	523.0
KPO_3–Ta $K_4P_2O_7$–Ta $(K_2CO_3 + P_2O_5)$–Ta	KPO_2	1 156.6	1 059.5	507.4
$(Rb_2CO_3 + P_2O_5)$–Ta	$RbPO_2$	1 159.3	1 058.2	501.3
$(Cs_2CO_3 + P_2O_5)$–Ta	$CsPO_2$	1 158.4	1 056.0	496.1
$(Na_2CO_3 + As_2O_3)$ $NaAsO_2$	$NaAsO_2$	853.2	868.2	418.0
$(K_2CO_3 + As_2O_3)$ $KAsO_2$	$KAsO_2$	852.6	865.4	409.2
$(Cs_2CO_3 + As_2O_3)$	$CsAsO_2$	851.5	863.0	393.0
$NaSb(OH)_6$	$NaSbO_2$	745.8	767.0	
$KSb(OH)_6$ $(K_2CO_3 + Sb_2O_3)$	$KSbO_2$	744.8	764.6	339.0
$(Cs_2CO_3 + Sb_2O_3)$	$CsSbO_2$	743.6 [b]	763.2 [c]	331.0

[a] Nitrogen matrices, frequency accuracy ± 0.5 cm^{-1}. [b] Mean of antimony isotope doublet at 744.0, 743.2 cm^{-1}. [c] Mean of antimony isotope doublet at 763.4, 762.9 cm^{-1}.
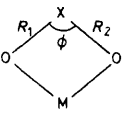
these remaining features are all expected to lie below 500 cm⁻¹. However, apart from the Li₃PO₄–Ta system where two bands at 302 and 311 cm⁻¹ are tentatively assigned to Li–O modes, our spectra showed little evidence of these fundamentals.

Finally, the effect of controlled diffusion and of varying the deposition rate was studied for several systems. In general, the intensities of the three

bending mode, the observation of the lowest frequency triplet at *ca.* 510 cm⁻¹ also permits a more rigorous quantitative analysis of the PO_2 unit.

The GVFF (general valence force field) for a C_{2v} triatomic species contains four independent parameters which may be defined by equation (1). In this expression, F_R and F_ϕ are the principal force constants associated with bond stretching and angle deformation, whilst F_{RR} and

TABLE 2

Observed and calculated frequencies (cm⁻¹) for isotopically labelled MXO_2 species

NaPO₂		CsAsO₂			KSbO₂			
Observed *	Calc. I	Observed *	Calc. II	Calc. III	Observed *	Calc. IV	Calc. V	Assignment
1 151.6	1 151.6	851.5	851.5	851.5	744.8	744.8	744.8	$MX^{18}O_2$ (B_2)
1 136.9	1 137.0	817.1	816.3	816.3	715.8	715.8	715.5⎫	$MX^{16}O^{18}O$
					713.8	713.8	713.5⎭	
1 113.9	1 113.7	814.1	814.2	814.2	708.4	708.3	708.3	$MX^{18}O_2$
1 062.1	1 062.1	863.0	863.0	863.0	764.6	764.6	764.6	$MX^{16}O_2$ (A_1)
1 035.4	1 035.3	857.7	857.6	857.6	757.8	757.8	757.9⎫	$MX^{16}O^{18}O$
					755.6	755.7	755.6⎭	
1 017.3	1 017.2	821.0	820.8	819.0	725.5	725.4	724.7	$MX^{18}O_2$
523.0	523.0	393.0	393.0		339.0	339.0		$MX^{16}O_2$ (A_1)
512.2	511.8	383.0	383.5		331.0	330.4		$MX^{16}O^{18}O$
500.6	500.4	374.0	373.9		323.0	321.5		$MX^{18}O_2$

Parameters used in calculations	Calc. I	Calc. II	Calc. III	Calc. IV	Calc. V
F_R/mdyn Å⁻¹	7.70	5.63	5.74	4.69, 4.71	4.73, 4.76
F_{RR}/mdyn Å⁻¹	0.46	0.39	0.50	0.23	0.28
F_ϕ/mdyn Å rad⁻²	1.87	1.95		1.94	
$F_{R\phi}$/mdyn rad⁻¹	0.27	−0.3		−0.24	
R/Å	1.5	1.8	1.8	2.0	2.0
ϕ/°	114	115	115	106	106

* Nitrogen matrices, frequency accuracy ±0.5 cm⁻¹.

fundamentals assigned to the PO_2 unit decreased during diffusion, and minor new features appeared close to the PO_2 bands. Thus for the sodium system, new bands were noted at 1 162, 1 155, 1 068, and 1 065 cm⁻¹, and the other alkali-metal phosphites produced similar shoulders. The appearance of such features has previously been noted in diffusion studies or KNO_3 [1] and $NaPO_3$,[2] where they were assigned as weak aggregates, and a similar explanation seems appropriate here. These bands were also observed in experiments employing low matrix ratios, but more significantly, all these experiments gave ' monomer ' PO_2 bands with the same relative intensities as found previously.

¹⁸O *enrichment in* $NaPO_2$. Our earlier report on the identification of $NaPO_2$ showed that ¹⁸O-enriched samples of sodium phosphate ultimately led to triplet patterns in the P–O stretching region characteristic of a species containing two equivalent oxygen atoms. Extension of these studies to cover the PO_2 bending mode reveals a similar triplet pattern. Figure 1(b) shows the three fundamentals assigned to $NaP^{16}O_2$, whilst Figure 1(c) shows the same spectral regions for the ¹⁸O-enriched material. The intensity ratios of the components in each triplet are the same, within experimental error, and correspond to *ca.* 26 atom % ¹⁸O enrichment in a species containing two equivalent oxygen atoms. The frequencies of these nine bands are listed in Table 2, together with their assignments, and in addition to confirming our identification of the A_1

$F_{R\phi}$ are interaction constants. These parameters, together with the bond angle, may all be evaluated from the

$$2V = F_R(\Delta R_1^2 + \Delta R_2^2) + 2F_{RR}\Delta R_1 \Delta R_2 + F_\phi\Delta_\phi^2 + 2F_{R\phi}\Delta_\phi(\Delta R_1 + \Delta R_2) \quad (1)$$

data for $NaP^{16}O_2$ and $NaP^{18}O_2$ using standard secular equations, and the additional frequencies available for the partially enriched species $NaP^{16}O^{18}O$ thus result in an overdetermination of the vibrational problem. A successful fit for all nine isotopic frequencies will therefore confirm our spectral assignments and also provide an estimate of the OPO bond angle.

The results of our GVFF calculations on the PO_2 unit in $NaPO_2$ are included in Table 2 (Calc. I) where the comparison with the experimental data is clearly very satisfactory. In these calculations, the bond angle OPO = 114° was obtained from the B_2 mode, and the attendant uncertainty arising from errors in frequency is *ca.* ±3°. This angle is somewhat smaller than that found in SO_2 (119.5°),[9] but rather similar to that in $H_2PO_2^-$ salts (*ca.* 116°).[10] However, our estimate neglects the effect of both anharmonicity and of vibrational coupling with low frequency cation motion and it would be realistic to place an uncertainty of ±5° on this value. The line diagram in Figure 1(d) summarises the results of these frequency calculations, and includes the expected relative band intensities for each of the three triplets, assuming two chemically equivalent oxygen

atoms and statistical abundances appropriate to 26 atom % ^{18}O enrichment. Any significant departure from equivalence between the two oxygen atoms would be revealed by a splitting of the central ($^{16}O^{18}O$) component of one or more of these triplets. The observed spectrum, however, shows no evidence of such a splitting for any of the fundamentals. Finally, it must be noted that although these results strongly indicate oxygen atom equivalence in $NaPO_2$, the experiments provide no method for distinguishing between the proposed C_{2v} structure and a lower symmetry structure in which, for example, the cation could lie in any position on the plane bisecting the OPO angle. This type of structural information will be difficult to establish from conventional high-temperature electron diffraction studies but might be possible using cooled beams.

$MAsO_2$ *Species.*—Figure 2(*a*) shows the nitrogen matrix spectrum obtained from the vaporisation of potassium arsenite ($KAsO_2$) at *ca.* 1 100 K contained in a platinum sample holder. Apart from the presence of CO_2, and traces of As_4O_6 (at *ca.* 829 cm^{-1}, denoted †)[11] these bands have not been observed before. Two of the new absorptions lie in the As–O stretching region, at 852.6 and 865.4 cm^{-1}, whilst the third occurs at 409.2 cm^{-1}, and by analogy with the MPO_2 systems reported above, these three bands are provisionally assigned to the AsO_2 modes in a C_{2v} cyclic species, $KAsO_2$. The same three bands could also be obtained from samples prepared by heating 1 : 1 mixtures of K_2CO_3 and As_2O_3 (see Experimental section), and parallel studies on the sodium and caesium systems yielded a similar pattern of new absorptions. The frequencies are summarised in Table 1. However, although the potassium and caesium systems produced only traces of As_4O_6, the vaporisation of either $NaAsO_2$, or samples derived from $Na_2CO_3 + As_2O_3$ mixtures, produced significant amounts of As_4O_6 in addition to the bands of interest. Several experiments were also carried out on mixtures of $Li_2CO_3 + As_2O_3$ but these regularly produced only As_4O_6, and no evidence was found for $LiAsO_2$ absorptions.

The initial assignment of the new bands as vibrations of the AsO_2 unit is supported firstly by comparison with the vibrational spectrum of monomeric SeO_2 and secondly by ^{18}O studies. In gas-phase SeO_2, the three fundamentals lie [12] at 967 (v_3, B_2), 923 (v_1, A_1), and at 368 cm^{-1} (v_2, A_1) and the bond angle has been accurately established [13] as OSeO = 113°50'. In low-temperature matrices, i.r. bands have been observed at 965.6, 922.0, and 372.5 cm^{-1} in argon,[14] with counterparts at 967.4, 928.4, and 371.9 cm^{-1} in nitrogen,[15] and in both these matrices, v_3 is significantly more intense in the i.r. than v_1. Our spectrum for $KAsO_2$ [Figure 2(*a*)] shows two closely spaced higher frequency bands, but in contrast to SeO_2, the more intense component lies at *lower* frequency. This suggests that in molecular $KAsO_2$, the A_1 As–O stretch lies above the more intense B_2 mode and the band assignments (Table 1) for our $MAsO_2$ modes are made on this basis. Confirmation of this assignment

comes from experiments on ^{18}O-enriched $CsAsO_2$. The caesium system was chosen for this study (in preference to the other cations) as it produced virtually no As_4O_6, and simple calculations had indicated that the presence of As_4O_6 would interfere with the ^{18}O isotope patterns expected for all the $MAsO_2$ systems.

Isotope Patterns for ^{18}O-*enriched* $CsAsO_2$.—The spectra obtained for ^{18}O-enriched $CsAsO_2$ show a total of nine bands. Three of these are found in the range 370—400
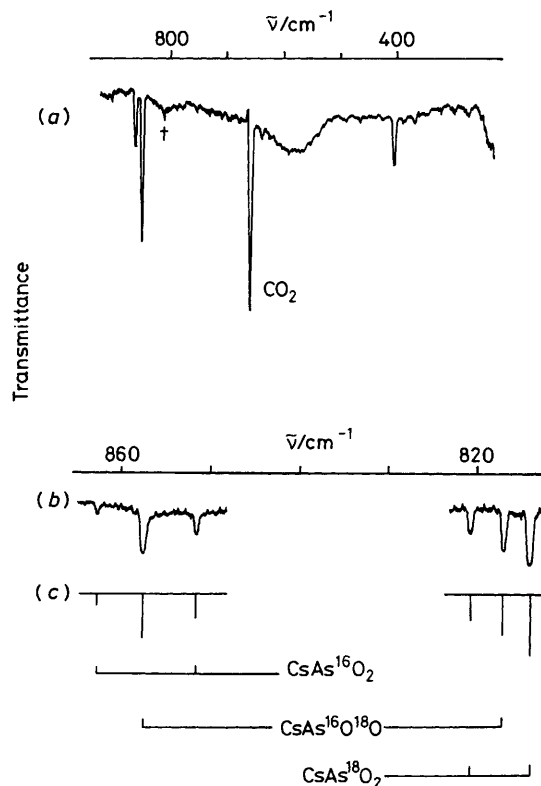

FIGURE 2 (*a*) N_2 matrix i.r. spectrum obtained from vaporisation of $KAsO_2$. (*b*) Infrared spectrum of the As–O stretching region for *ca.* 63 atom % ^{18}O-enriched $CsAsO_2$. (*c*) Calculated spectrum

cm^{-1}, and by comparison with the $NaPO_2$ data are readily assigned as the bending modes of the AsO_2 unit in $CsAs^{16}O_2$, $CsAs^{16}O^{18}O$, and $CsAs^{18}O_2$ (Table 2). The remaining six bands occur in the As–O stretching region, but their interpretation is not as straightforward. Figure 2(*b*) shows the spectrum obtained from this system with an ^{18}O isotope enrichment of *ca.* 63 atom %. At first glance it would appear to consist of two triplets similar to those found for ^{18}O-enriched $NaPO_2$. However, comparison with the pure ^{16}O data shows that the upper triplet includes *both* the A_1 and B_2 modes of $CsAs^{16}O_2$ rather than one band from each isotopomer. These both shift by *ca.* 40 cm^{-1} to give $CsAs^{18}O_2$ counterparts at 814.1 and 821.0 cm^{-1} and the bands due to $CsAs^{16}O^{18}O$ are assigned at 817.1 and 857.7 cm^{-1}. The frequency separation between these mixed isotope bands is *ca.* 40 cm^{-1} and is thus significantly greater than the

A_1–B_2 separations of *ca.* 10 cm^{-1} in the isotopically pure species. In CsAs^{16}O^{18}O the two As–O stretching modes have evidently interacted strongly and Figure 2(*b*) shows that as a result of this there has also been significant intensity borrowing by the 857.7 cm^{-1} component at the expense of its partner. Qualitatively, this might have been anticipated, as the ^{16}O–^{18}O isotope shifts in this system were estimated to be larger than the A_1–B_2 frequency difference, but it is important to confirm this interpretation using a more quantitative approach.

Two models were chosen in order to obtain a spectral fit for this ^{18}O data. Firstly, a GVFF analysis was carried out for the bent AsO$_2$ unit in an attempt to fit the nine fundamentals observed in the mixed isotope experiment. A comparison between the observed frequencies and those calculated using this model (Calc. II) is available from Table 2, and the agreement is very satisfactory. However, this analysis does not lend itself easily to a corresponding treatment of band intensities, and in order to simulate the intensity borrowing in CsAs^{16}O^{18}O a second set of calculations was performed in which the As–O stretching modes are factored off from the remaining vibrations of the molecule. Only two parameters are therefore retained in the corresponding force field [equation (2)]. Provided that these two

$$2V = F_{\mathrm{R}}(\Delta R_1{}^2 + \Delta R_2{}^2) + 2F_{\mathrm{RR}}\Delta R_1 \Delta R_2 \quad (2)$$

force constants adequately reproduce the stretching frequency data the principal advantage of this approach is that it then allows the calculation of the relative intensities of all six components assuming only the general validity of the bond dipole model for i.r. intensities.[16] No additional specific parameters are necessary.

The appropriate secular equations for the two stretching modes in a bent species of type YXY' (*e.g.* the As–O stretching modes in CsAs^{16}O^{18}O) are (3) and (4). In

$$\lambda_1 + \lambda_2 = F_{\mathrm{R}}(G_{11} + G_{22}) + 2F_{\mathrm{RR}}G_{12} \quad (3)$$

$$\lambda_1\lambda_2 = (F_{\mathrm{R}}{}^2 - F_{\mathrm{RR}}{}^2)(G_{11}G_{22} - G_{12}G_{21}) \quad (4)$$

these equations $G_{11} = \dfrac{1}{M_{\mathrm{X}}} + \dfrac{1}{M_{\mathrm{Y}}}$, $G_{22} = \dfrac{1}{M_{\mathrm{X}}} + \dfrac{1}{M_{\mathrm{Y}}}$, and $G_{12} = G_{21} = \dfrac{\cos\phi}{M_{\mathrm{X}}}$, where ϕ is the angle YXY', and M_{X} and M_{Y} denote the masses of atoms X and Y. If the usual assumption is made that $\lambda = 4\pi^2 c^2 \nu^2$, where ν is the observed vibrational transition (in cm^{-1}), these two equations will generate the As–O stretching frequencies of CsAs^{16}O$_2$, CsAs^{16}O^{18}O, and CsAs^{18}O$_2$ using only F_{R}, F_{RR}, and ϕ as independent variables. The results of this model (Calc. III) are included in Table 2, and it is interesting to note that this simpler force field is only marginally less successful than the GVFF in reproducing the observed stretching modes. The values of F_{R} and F_{RR} are very similar to the corresponding parameters in the GVFF indicating that the separation of stretching and bending modes in this molecule is a relatively harmless approximation, and this in turn suggests that

the relative intensities of these stretching modes might be predicted using the simple bond dipole approach.

For the two stretching modes considered here, the general expressions [16] (5) and (6) may be simplified to (7) and (8). Here I_1 and I_2 may be termed ' intrinsic

$$\Sigma I_{\mathrm{k}} = \Sigma\, \frac{\partial\mu}{\partial S_{\mathrm{k'}}} \cdot \frac{\partial\mu}{\partial S_{\mathrm{k''}}} \cdot G_{\mathrm{k'k''}} \quad (5)$$

$$\Sigma\, \frac{I_{\mathrm{k}}}{\lambda_{\mathrm{k}}} = \Sigma\, \frac{\partial\mu}{\partial S_{\mathrm{k'}}} \cdot \frac{\partial\mu}{\partial S_{\mathrm{k''}}} \cdot F_{\mathrm{k'k''}}{}^{-1} \quad (6)$$

$$I_1 + I_2 = G_{11} + G_{22} + 2G_{12}\cos\phi \quad (7)$$

$$\frac{I_1}{\lambda_1} + \frac{I_2}{\lambda_2} = (2F_{\mathrm{R}} - 2F_{\mathrm{RR}}\cos\phi)/(F_{\mathrm{R}}{}^2 - F_{\mathrm{RR}}{}^2) \quad (8)$$

intensities ', and correspond to the relative intensities of the two stretching modes for a given isotopomer. In order to predict the relative intensities in a mixture of isotopomers, these values must be weighted according to the appropriate statistical abundances. The line diagram in Figure 2(*c*) shows how useful this simple model turns out to be. Not only is the frequency fit satisfactory, but the model has been surprisingly successful in predicting both the relative intensities of the A_1 and B_2 modes in CsAs^{16}O$_2$ and CsAs^{18}O$_2$, and also the extent of intensity borrowing in CsAs^{16}O^{18}O. The OAsO bond angle is estimated to be *ca.* 115° from these analyses, and the uncertainties in frequency associated with the B_2 stretching modes (*ca.* 0.5 cm^{-1}) lead to an estimated error in bond angle of *ca.* ±4°.

MSbO$_2$ Species.—Figure 3(*a*) shows the nitrogen matrix spectrum obtained from the vaporisation of a K$_2$CO$_3$–Sb$_2$O$_3$ mixture at *ca.* 1 200 K. In addition to the CO$_2$ absorption at *ca.* 662 cm^{-1}, this spectrum shows three prominent bands at 744.8, 764.6, and 339.0 cm^{-1}, and these same new bands were also obtained from samples of KSb(OH)$_6$ which had been preheated to remove water. The similarity with the spectrum previously obtained from K$_2$CO$_3$–As$_2$O$_3$ mixtures suggests that these three bands correspond to SbO$_2$ modes in the analogous species KSbO$_2$. Two much weaker features (denoted by a cross) are also present in Figure 3(*a*) at 734 and 569 cm^{-1}, but comparison between several different experiments revealed a variable-intensity behaviour of these bands with respect to those attributed to KSbO$_2$, and they remain unassigned.

Corresponding studies on the sodium and caesium systems yielded similar bands, with only minor frequency shifts, and the results of all these experiments are summarised in Table 1, together with suggested assignments based on a C_{2v} SbO$_2$ unit. The vaporisation of Li$_2$CO$_3$–Sb$_2$O$_3$ mixtures under similar conditions produced only Sb$_4$O$_6$.

^{18}O *enrichment in* KSbO$_2$. The effect of ^{18}O enrichment on these antimony systems was qualitatively very similar to that found for CsAsO$_2$. In particular, low-resolution studies on samples of ^{18}O-enriched KSb(OH)$_6$ produced a simple triplet in the SbO$_2$ bending region (at 339, 331, and 323 cm^{-1}) and a complex pattern of six

bands for the Sb–O stretching modes. Under higher resolution, however, two of these latter bands could be resolved into doublets giving a total of eight components, and a typical spectrum is shown in Figure 3(b). The degree of enrichment in this experiment was ca. 67 atom % ^{18}O, and the assignment of this spectrum in terms of
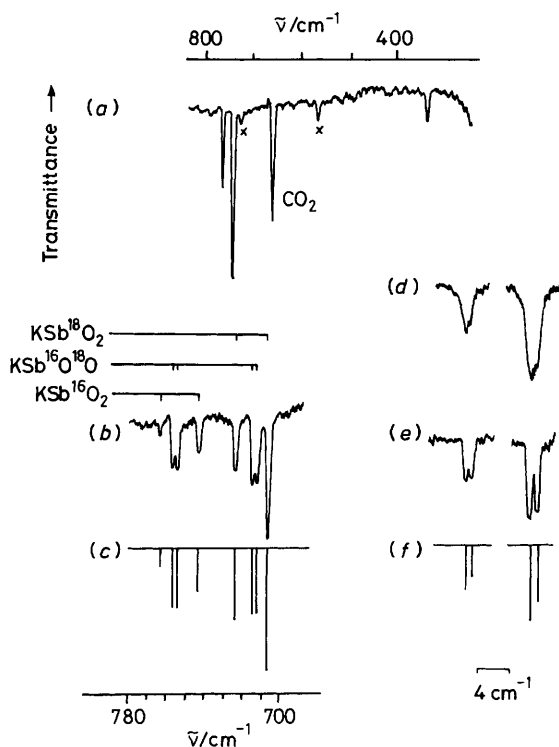

FIGURE 3 (a) N_2 matrix i.r. spectrum obtained from vaporisation of a solid mixture of $K_2CO_3 + Sb_2O_3$. (b) Infrared spectrum of the Sb–O stretching region for ca. 67 atom % ^{18}O-enriched $KSbO_2$. (c) Calculated spectrum. (d) Sb–O stretching modes in $KSb^{16}O_2$ under higher resolution. (e) Sb–O stretching modes in $CsSb^{16}O_2$ showing partially resolved doublets. (f) Calculated antimony isotope fine structure in $CsSb^{16}O_2$

the various isotopomers of $KSbO_2$ is relatively straightforward (Table 2). Comparison with the data on $CsAsO_2$ indicates that it is the mixed species $KSb^{16}O^{18}O$ which gives rise to the two doublets [Figure 3(b)] and this suggests that the two Sb–O bonds in $KSbO_2$ are not strictly equivalent. Two sets of calculations were therefore carried out to clarify the position.

The first approach was to attempt to reproduce all eleven frequencies observed for this mixture of isotopomers using a GVFF calculation. The inequivalence between the Sb–O bonds was simulated by allowing two different principal stretching constants, but apart from this minor change, the analysis was identical to that performed on $CsAsO_2$. The results of these frequency calculations are summarised under Calc. IV in Table 2, and the agreement with the observed bands is very satisfactory. As in the case of $CsAsO_2$, the bond angle OSbO is treated as a variable parameter in the analysis, and the value which emerges for $KSbO_2$ is 106°. The estimated error limits based on frequency uncertainties

in the B_2 modes are ca. $\pm 5°$, and it is interesting to note that this angle has a similar value to that estimated for TeO_2 (ca. 110°) isolated in low-temperature matrices.[17]

One of the more significant features of the $CsAsO_2$ system was the mutual interaction of the two As–O stretches in $CsAs^{16}O^{18}O$, and Figure 3(b) shows that a similar phenomenon is present in $KSbO_2$. Although the frequency perturbation is satisfactorily reproduced by the GVFF approach, it seemed worthwhile to attempt an intensity fit using the same approach as for $CsAsO_2$. The frequencies calculated using this simple force field are included in Table 2 under Calc. V, and our relative intensity predictions for 67 atom % ^{18}O enrichment are shown in Figure 3(c). In this diagram, we have assumed that the total intensity expected for the $KSb^{16}O^{18}O$ bands is distributed equally between the components of each doublet. Both models therefore strongly support our original assignment of these bands as fundamentals of a bent SbO_2 unit, and this raises two important points. The first concerns the apparent inequivalence of the two Sb–O bonds, and the second poses the question as to whether any of these fundamentals should show a resolvable antimony isotope effect.

Both vibrational analyses indicate a relatively small difference (ca. 0.6%) between the two principal Sb–O stretching constants. This could represent either a genuine distortion from presumed C_{2v} symmetry such that this inequivalence persists in the free molecule, or alternatively it could arise from a perturbation induced by the matrix environment; for example, by trapping in a low symmetry site. As indicated earlier, argon matrix spectra unfortunately showed complex absorptions for the parent $KSb^{16}O_2$ modes, and would therefore be of little help. We therefore chose instead to carry out two ^{18}O-enrichment experiments on $CsSbO_2$ to see whether this apparent inequivalence was a general feature of $MSbO_2$ systems.

^{18}O enrichment in $CsSbO_2$. The product obtained from the fusion of Cs_2CO_3 with Sb_2O_3 was found to be virtually insoluble in water, but after several weeks contact with $H_2^{18}O$ in a sealed tube was found to have undergone ^{18}O exchange to a limited extent. The nitrogen matrix spectrum obtained from the vaporisation of this material showed four prominent Sb–O stretching frequencies at 763.2, 743.6, 755.4, and 713.5 cm^{-1}. Two of these correspond to the $CsSb^{16}O_2$ fundamentals assigned earlier (Table 1) whilst those at 755.4 and 713.5 cm^{-1} are assigned to $CsSb^{16}O^{18}O$ by comparison with the positions of the doublets in $KSb^{16}O^{18}O$ (Table 2). The two bands of $CsSb^{18}O_2$ in this region could not be located with any confidence owing to the low degree of enrichment. Examination of these four bands at a spectral slit-width of 1.4 cm^{-1} revealed no band splittings, and $CsSbO_2$ would therefore appear to contain equivalent Sb–O bonds. The splitting observed in the $KSb^{16}O^{18}O$ bands (ca. 2 cm^{-1}) does not therefore appear to be a general feature of $MSbO_2$ systems and in view of the small difference in principal force constants required to simulate this splitting, we consider it to be a matrix

perturbation caused by trapping on a low-symmetry site.

Antimony Isotope Effects.—Naturally occurring antimony consists of two isotopes, ^{121}Sb (57.3%) and ^{123}Sb (42.7%), and it may readily be shown that in a bent SbO_2 unit with OSbO *ca.* 106°, the resulting isotope splittings expected on Sb–O stretching modes at *ca.* 750 cm^{-1} are in the range 0.5—1.0 cm^{-1}. Examination of our $KSb^{16}O_2$ spectra in this region under optimum resolution conditions (typically *ca.* 0.5 cm^{-1}), however, yielded rather broad singlets. A typical spectrum is shown in Figure 3(*d*). However, at a resolution of better than *ca.* 1 cm^{-1}, the caesium system began to show evidence of band splitting, and at a spectral slit-width of 0.4 cm^{-1}, the spectrum shown in Figure 3(*e*) was obtained. Here, the upper (A_1) fundamental at 763.2 cm^{-1} appears as a doublet with a separation of *ca.* 0.5 cm^{-1}, whilst the mode at 743.6 cm^{-1} is split by *ca.* 0.8 cm^{-1} (Table 1).

Although it is possible that these splittings arise from matrix effects, we believe that they are in fact due to the two antimony isotopes. This assignment is supported by a calculation of the ^{121}Sb–^{123}Sb splitting for each fundamental using the two-parameter force field described earlier. Figure 3(*f*) shows the positions and relative intensities of the antimony isotope doublets expected for an SbO_2 unit with a bond angle of 106° where the principal and interaction stretching constants have values of 4.74 and 0.27 mdyn Å^{-1} respectively.* The agreement is very satisfactory, and in addition to confirming the presence of one atom of antimony, these splittings are also consistent with our assignment of the symmetric and asymmetric modes.

CONCLUSIONS

The results described in this paper are consistent with the isolation of new high-temperature molecular species MXO_2, where M is an alkali metal and X = P, As, or Sb. However, although our isotope experiments and vibrational analyses provide convincing evidence for the presence of XO_2 units, there is little direct indication of the presence of an alkali metal in these species. Only in $LiPO_2$ were we able to observe bands which might be assigned to cation motion, and for the remaining species, the presence of the alkali metal was inferred from the cation dependence of the XO_2 frequencies. It is therefore important to inquire whether the presence of an alkali metal is confirmed by other studies.

The only experiments to date which indicate directly the presence of an alkali metal in any of these molecules are the mass-spectrometric studies on phosphates reported by Gingerich and Miller.[18] As discussed in our earlier note,[3] this mass-spectrometric work involved the vaporisation of sodium phosphate under potentially

* Throughout this paper: 1 dyn = 10^{-5} N.

reducing conditions, and a prominent ion current was noted for $NaPO_2^+$. This was believed to originate from a neutral $NaPO_2$ precursor, and it was also found that ion currents for binary species $P_xO_y^+$ were relatively low. The evidence for alkali-metal transport in this system is therefore fairly conclusive, and we visualise an essentially ionic structure $Na^+\left(\begin{smallmatrix}O\\O\end{smallmatrix}\!\!>\!\!P\right)^-$ for this molecule.

Corresponding mass-spectrometric studies on the arsenic and antimony systems do not appear to have been carried out, but we believe that essentially ionic MXO_2 ring structures are similarly present in these systems, and provide the best interpretation of our spectroscopic data. Although the OAsO and OSbO angles which emerge from these analyses inevitably carry fairly large error limits (*ca.* ±5°) as a result of experimental uncertainties and approximations in the vibrational model, these angles are similar to those previously reported in SeO_2 and TeO_2 respectively. The decrease in bond angle from As (or Se) to Sb (or Te) may be chemically significant, and would be consistent with a decreasing involvement of s orbitals in the σ system.

REFERENCES

[1] See for example, I.R. Beattie, J. S. Ogden, and D. D. Price, *J. Chem. Soc., Dalton Trans.*, 1979, 1460; J. S. Ogden and S. J. Williams, *ibid.*, 1981, 456.
[2] S. N. Jenny and J. S. Ogden, *J. Chem. Soc., Dalton Trans.*, 1979, 1465.
[3] J. S. Ogden and S. J. Williams, *J. Chem. Phys.*, 1980, **73**, 2007.
[4] See for example, J. R. Van Wazer, ' Phosphorus and its Compounds,' Interscience, New York, 1958, vol. 1, p. 279.
[5] I. R. Beattie, H. E. Blayden, S. M. Hall, S. N. Jenny, and J. S. Ogden, *J. Chem. Soc., Dalton Trans.*, 1976, 666.
[6] See for example, W. Levason, R. Narayanaswamy, J. S. Ogden, A. J. Rest, and J. W. Turff, *J. Chem. Soc., Dalton Trans.*, 1981, 2501.
[7] R. D. Shelton, A. H. Nielsen, and W. H. Fletcher, *J. Chem. Phys.*, 1953, **21**, 2178.
[8] M. Abenoza and V. Tabacik, *J. Mol. Struct.*, 1975, **26**, 95.
[9] M. H. Sirvetz, *J. Chem. Phys.*, 1951, **19**, 938.
[10] J. L. Galigne and Y. Dumas, *Acta Crystallogr., Sect. B*, 1973, **29**, 1115.
[11] S. N. Jenny, Ph.D. Thesis, University of Southampton, 1981.
[12] P. A. Giguere and M. Falk, *Spectrochim. Acta*, 1960, **16**, 1; D. Boal, G. Briggs, H. Huber, G. A. Ozin, E. A. Robinson, and A. Vander Voet, *Chem. Commun.*, 1971, 686.
[13] H. Takeo, E. Hirota, and Y. Morino, *J. Mol. Spectrosc.*, 1970, **34**, 370.
[14] S. N. Cesaro, M. Spoliti, A. J. Hinchcliffe, and J. S. Ogden, *J. Chem. Phys.*, 1971, **55**, 5834; J. W. Hastie, R. Hauge, and J. L. Margrave, *J. Inorg. Nucl. Chem.*, 1969, **31**, 281.
[15] A. J. Hinchcliffe, D.Phil. Thesis, University of Oxford, 1971.
[16] See for example, E. B. Wilson, jun., J. C. Decius, and P. C. Cross, ' Molecular Vibrations,' McGraw-Hill, New York, 1955, pp. 166 and 192.
[17] D. W. Muenow, J. W. Hastie, R. Hauge, R. Bautista, and J. L. Margrave, *Trans. Faraday Soc.*, 1969, **65**, 3210.
[18] K. A. Gingerich and F. Miller, *J. Chem. Phys.*, 1975, **63**, 1211.